

Magneto-optical spectroscopy of two-dimensional holes in GaAs/Al_xGa_{1-x}As single heterojunctions

O. V. Volkov, V. E. Zhitomirskii, and I. V. Kukushkin

*Max-Planck-Institut für Festkörperforschung, Heisenbergstrasse, 1, D-70569 Stuttgart, Germany
and Institute of Solid State Physics, RAS, Chernogolovka, 142432 Russia*

W. Dietsche, K. v. Klitzing, A. Fischer, and K. Eberl

*Max-Planck-Institut für Festkörperforschung, Heisenbergstrasse, 1, D-70569 Stuttgart, Germany
(Received 17 March 1997)*

The energy spectrum of two-dimensional (2D) holes in a perpendicular magnetic field is investigated in *p*-type GaAs/AlGaAs single heterojunctions using a magneto-optical method based on the study of radiative recombination of 2D holes with photoexcited electrons bound to donors. A complex structure of both heavy- and light-hole energy levels is directly observed in luminescence spectrum, and the magnetic-field dependencies of the energy splittings between different quantum states of the 2D holes is studied using an analysis of circular polarization of the magnetoluminescence. The experimental results are compared with the energy spectrum of 2D holes calculated with the use of the 4×4 Luttinger $k \cdot p$ Hamiltonian and a reasonable agreement is established. [S0163-1829(97)04536-0]

I. INTRODUCTION

During the last few decades the fundamental physical phenomena found in two-dimensional (2D) systems have attracted considerable interest. Integral and the fractional quantum Hall effects and Wigner crystallization were observed in these systems¹⁻³ and stimulated intensive experimental and theoretical activities. Different experimental techniques (such as magnetotransport, FIR spectroscopy, Raman spectroscopy, microwave spectroscopy, magneto-optics, and others) were used to study the energy spectrum of the 2D system in a perpendicular magnetic field. While the properties of 2D electrons were intensively studied and rather well understood by these methods, much less information was established for 2D hole systems. This is mainly due to the fact that the hole mass is much heavier than the electron mass and because the nonparabolicity and valence band anisotropy result in a much more complicated energy spectrum for the 2D holes in comparison with the 2D electron spectrum. It was demonstrated by several theoretical calculations⁴⁻⁶ that the Landau levels of the holes are not equidistant and are strongly nonlinear as a function of the magnetic field. However, this complicated behavior was never directly observed experimentally. Moreover, a trivial, electronlike energy spectrum (with equidistant spin split Landau levels) was used for an explanation of the transport results in most publications.⁷ Magneto-optical investigations of the energy spectrum of 2D holes performed previously deal either with extreme magnetic field limit⁸ or with 2D electron-free-hole recombination in *n*-type doped quantum well structures.⁹ In the latter case an optical method is usually used to study properties of 2D electrons and of empty 2D hole levels. However, the analysis of such experimental data is rather difficult because of strong Coulomb interaction between electrons and holes confined in the same potential well.

The progress in technology substantially improves the quality of the *p* channels in GaAs/AlGaAs heterojunctions [especially for the structures grown on nonconventional sur-

faces such as the (311) surface¹⁰] and almost all intriguing phenomena found for the 2D electron system were also observed in 2D hole channels.¹¹⁻¹³ These observations stimulate further investigations of the energy spectrum of 2D holes in a perpendicular magnetic field. One of the most powerful methods to study the energy spectrum of 2D electrons is based on the investigation of radiative recombination of two-dimensional electrons with photoexcited holes bound to acceptors. This technique was used to study the energy spectrum of electrons under the conditions of the integer and fractional quantum Hall effect (FQHE)¹⁴ and is based on the fact that the recombination probability of electrons is independent of the energy of electrons associated with in-plane motion and therefore, the intensity of luminescence directly reflects the single particle density of states of 2D electrons. As a result, the shape of the luminescence line, measured at zero magnetic field has a rectangular form with a width equal to the Fermi energy of the 2D electrons. In a perpendicular magnetic field the splitting of the density of states into Landau levels was directly observed in the luminescence spectra,¹⁴ and this method was also very effective for the determination of the spin splitting and of the energy gaps under the conditions of the FQHE.¹⁵ The key point which distinguishes the cases of 2D electrons and of 2D holes is that the in-plane motion of 2D electrons can be separated in the Hamiltonian from the motion in the perpendicular direction (also in a perpendicular magnetic field), whereas it is not valid for 2D holes. Therefore, there is no reason to expect that the spectra of radiative recombination of 2D holes with photoexcited electrons bound to donors will reflect the energy spectrum of the holes, nevertheless, it should be possible to distinguish between different quantum states of 2D holes and to measure the splitting between them. However, to do this we will need quantitative comparison with theoretical calculation, which will include comparison of intensities, polarization, and the energy splittings between different lines.

In the present paper we investigated specially designed *p*-type GaAs/AlGaAs single heterojunctions with a monolayer of donors, located at a well defined distance in the GaAs buffer layer. Radiative recombination of 2D holes with photoexcited electrons bound to donors is studied with the analysis of circular polarization. To derive the energy spectrum of 2D holes from the luminescence spectrum we compare the experimental data with the results of calculations performed with the use of a 4×4 Luttinger *k*·*p* Hamiltonian with the potential well found self-consistently in the Hartree approximation by solving Poisson's equation numerically. A complex structure of Landau levels of both heavy and light holes is established in luminescence spectra and the magnetic field dependencies of the energy splittings between different quantum states is measured. The magnetic field dependencies of the intensity, polarization, and energy splitting of different lines are compared with the results of calculations and a reasonable agreement is established.

II. EXPERIMENTAL TECHNIQUE

We studied several *p*-type GaAs/Al_{*x*}Ga_{*1-x*}As single heterojunctions with a δ -doped monolayer of Si donors ($n_D = 2 \times 10^{10} \text{ cm}^{-2}$) located in a wide ($1 \mu\text{m}$) GaAs buffer layer at a well-defined distance Z_0 from the interface. We studied the samples in which Z_0 was equal to 25, 30, 35, 40, 45, and 55 nm. Structures were grown on the (100) surface of GaAs substrates with the use of carbon (10^{18} cm^{-3}) as a *p* dopant of the AlGaAs layer (the width of the spacer layer was 20 nm). The concentration and the mobility of 2D holes were in the range of $(2.5-5) \times 10^{11} \text{ cm}^{-2}$ and $(50-90) \times 10^3 \text{ cm}^2/\text{V s}$, respectively. For photoexcitation, we used a tunable Ti-sapphire laser (wavelength $\sim 800 \text{ nm}$) with a power density of about 10^{-2} W/cm^2 . Luminescence spectra were detected by CCD camera and double spectrometer Ramanor U-1000 (spectral resolution was about 0.03 meV). To analyze circular polarization of the luminescence we used an optical fiber system with quarter-wave plate and a linear polarizer located just above the sample (the σ^+ and σ^- components of luminescence were obtained with differ-

ent orientations of the perpendicular magnetic field). The 2D-hole concentration was determined using magnetotransport measurements on the same samples with and without laser illumination.

III. COMPUTATIONAL DETAILS

In order to understand which states of 2D holes are responsible for the observed optical transitions we performed calculations of the energy spectrum of 2D holes in a perpendicular magnetic field which also allowed us to know the magnetic field dependence of the recombination intensity and of the degree of circular polarization. The energy spectrum of 2D holes in perpendicular magnetic field was calculated by many authors.⁴⁻⁶ Usually all calculations were performed by the matrix method, which is based on the Hamiltonian diagonalization on the limited basis functions set. The precision of such methods is strongly dependent on the choice of the basic functions set and there is a problem with its estimation. The task becomes especially complicated in the case of self-consistent calculation of the electrostatic potential screened by the hole gas itself due to the fact that holes wave functions are not separable in the direction normal to the well and that they are strongly affected by the external magnetic field. In contrast to the matrix method we have developed another technique which is based on the Hamiltonian transformation into the system of first order nonlinear differential equations. This procedure allows us to obtain holes wave functions, energy eigenvalues, and potential slope simultaneously without additional iterations. For solving a total system of first order differential equations including Schrödinger and Poisson equations we perform spatial discretization with variable step. The system of nonlinear final difference equations then can be easily solved using relaxation method¹⁶ which is a realization of Newton iterations for such a system.

Following Ref. 6 we consider a 4×4 Luttinger Hamiltonian in the cylindrical approximation in which linear *k* terms are neglected:

$$\mathbf{H} = \begin{vmatrix} P+Q - \frac{3}{2} \frac{e}{c} KB & S^+ & R^+ & 0 \\ S & P-Q - \frac{1}{2} \frac{e}{c} KB & 0 & R^+ \\ R & 0 & P-Q + \frac{1}{2} \frac{e}{c} KB & -S^+ \\ 0 & R & -S & P+Q + \frac{3}{2} \frac{e}{c} KB \end{vmatrix}, \quad (1)$$

where

$$P = \frac{\gamma_1}{2}(k_z^2 + k^2), \quad k_{\pm} = k_x \pm ik_y,$$

$$Q = \frac{\gamma_2}{2}(-2k_z^2 + k^2), \quad k^2 = k_x^2 + k_y^2,$$

$$R = -\frac{\sqrt{3}}{2}\bar{\gamma}k_z^2 + \frac{\sqrt{3}}{2}\mu k_+^2, \quad \bar{\gamma} = \frac{1}{2}(\gamma_3 + \gamma_2),$$

$$S = \sqrt{3}\gamma_3 k_z k_-, \quad \mu = \frac{1}{2}(\gamma_3 - \gamma_2).$$

Here we use slightly different consideration on energy and wave function components then.⁶ The light emission we treat as annihilation of the electron-hole pair which has the total momentum equal to photon momentum (± 1 for circular polarized light). Thus the energy of the holes states in our consideration has the opposite sign in comparison with Ref. 6, where the electron transitions from hole- to electron-type states were considered. We also use a different order of spin components which are more natural in our opinion:

$$\vec{\Phi} = \begin{pmatrix} \phi_{-3/2} \\ \phi_{-1/2} \\ \phi_{+1/2} \\ \phi_{+3/2} \end{pmatrix},$$

where the index designates the spin projection on the z axis.

As usual, we introduce magnetic field in the Hamiltonian by the substitution

$$k_{\alpha} = \frac{1}{i} \frac{\partial}{\partial x_{\alpha}} + \frac{e}{\hbar c} A_{\alpha},$$

where A_{α} is the magnetic field vector potential. Then

$$[k_{\alpha}, k_{\beta}] = \frac{1}{i} \frac{e}{\hbar c} \left(\frac{\partial A_{\beta}}{\partial x_{\alpha}} - \frac{\partial A_{\alpha}}{\partial x_{\beta}} \right) = \frac{1}{i} \frac{e}{\hbar c} (\nabla \times A)_{\gamma} = \frac{1}{i} \frac{e}{\hbar c} B_{\gamma}.$$

In our case B is along the z direction, hence

$$[k_x, k_z] = [k_y, k_z] = 0, \quad [k_x, k_y] = \frac{1}{i} \frac{eB}{\hbar c} = \frac{1}{il^2},$$

where

$$l = \left(\frac{\hbar c}{eB} \right)^{1/2}$$

is the magnetic length.

Let us introduce ladder operators

$$a^+ = \frac{l}{\sqrt{2}} k_+ a = \frac{l}{\sqrt{2}} k_- N = a^+ a,$$

which satisfy the relation

$$[a, a^+] = il^2 [k_x, k_y] = 1.$$

Hence the N operator has the eigenvalues $0, 1, 2, \dots$. Let us denote them by s_0, s_1, s_2, \dots , then we can obtain the relations

$$a^+ s_{n-1} = \sqrt{n} s_n a s_n = \sqrt{n} s_{n-1}. \quad (2)$$

Now we can rewrite the Hamiltonian in terms of ladder operators, neglecting the anisotropy term in R (containing μ), that allow us to write the solution vector in a finite basis. We have

$$\begin{aligned} N = a^+ a &= \frac{l^2}{2} (k_x + ik_y)(k_x - ik_y) = \frac{l^2}{2} (k^2 + i[k_y, k_x]) \\ &= \frac{l^2}{2} k^2 - \frac{1}{2}. \end{aligned}$$

Hence,

$$P = \frac{\gamma_1}{2} \left[k_z^2 + \frac{1}{l^2} (2N + 1) \right], \quad R = -\sqrt{3} \bar{\gamma} \frac{1}{l^2} a^2,$$

$$Q = \frac{\gamma_2}{2} \left[-2k_z^2 + \frac{1}{l^2} (2N + 1) \right], \quad S = \sqrt{6} \gamma_3 k_z \frac{1}{l} a.$$

Then

$$P \pm Q = \left(\frac{\gamma_1}{2} \mp \gamma_2 \right) k_z^2 + \left(\frac{\gamma_1}{2} \pm \frac{\gamma_2}{2} \right) \frac{1}{l^2} (2N + 1).$$

Let us denote

$$m_h = \left(\frac{\gamma_1}{2} - \gamma_2 \right)^{-1}, \quad m_l = \left(\frac{\gamma_1}{2} + \gamma_2 \right)^{-1},$$

$$A = \gamma_1 + \gamma_2, \quad B = \gamma_1 - \gamma_2,$$

$$r = \sqrt{3} \bar{\gamma}, \quad s = \sqrt{\frac{3}{2}} \gamma_3,$$

where m_h, m_l represent two times the effective masses of heavy and light holes. Now we can write the Hamiltonian (1) in the form

$$\mathbf{H} = \begin{pmatrix} \frac{k_z^2}{m_h} + \frac{A}{l^2} \left(N + \frac{1}{2} \right) - \frac{3K}{2l^2} & \frac{2s}{l} k_z a^+ & -\frac{r}{l^2} a^{+2} & 0 \\ \frac{2s}{l} k_z a & \frac{k_z^2}{m_l} + \frac{B}{l^2} \left(N + \frac{1}{2} \right) - \frac{1K}{2l^2} & 0 & -\frac{r}{l^2} a^{+2} \\ -\frac{r}{l^2} a^2 & 0 & \frac{k_z^2}{m_l} + \frac{B}{l^2} \left(N + \frac{1}{2} \right) + \frac{1K}{2l^2} & -\frac{2s}{l} k_z a^+ \\ 0 & -\frac{r}{l^2} a^2 & -\frac{2s}{l} k_z a & \frac{k_z^2}{m_h} + \frac{A}{l^2} \left(N + \frac{1}{2} \right) + \frac{3K}{2l^2} \end{pmatrix}. \quad (3)$$

We will find the solution in the form

$$\vec{\Phi} = \begin{pmatrix} s_n(x, y) * \psi_1(z) \\ -i s_{n-1}(x, y) * \psi_2(z) \\ -s_{n-2}(x, y) * \psi_3(z) \\ i s_{n-3}(x, y) * \psi_4(z) \end{pmatrix},$$

where, s_n are the in-plane Landau level n envelope functions and the eigenfunctions of the N operator ψ_i are z -dependent envelope functions corresponding to different spin projections. Using relations (2) the Hamiltonian (3) can be rewritten as a matrix acting upon $\psi_i(z)$ functions only:

$$\mathbf{H} = \begin{pmatrix} -\frac{1}{m_h} \frac{\partial^2}{\partial z^2} + E_0 & -\frac{2Q}{l} \frac{\partial}{\partial z} & \frac{N}{l^2} & 0 \\ \frac{2Q}{l} \frac{\partial}{\partial z} & -\frac{1}{m_l} \frac{\partial^2}{\partial z^2} + E_1 & 0 & \frac{M}{l^2} \\ \frac{N}{l^2} & 0 & -\frac{1}{m_l} \frac{\partial^2}{\partial z^2} + E_2 & \frac{2P}{l} \frac{\partial}{\partial z} \\ 0 & \frac{M}{l^2} & -\frac{2P}{l} \frac{\partial}{\partial z} & -\frac{1}{m_h} \frac{\partial^2}{\partial z^2} + E_3 \end{pmatrix}, \quad (4)$$

where we have substituted $k_z \rightarrow 1/i \partial/\partial z$ and denoted

$$M = r\sqrt{(n-1)(n-2)}, \quad N = r\sqrt{n(n-1)},$$

$$P = s\sqrt{n-2}, \quad Q = s\sqrt{n},$$

$$E_0 = \frac{A}{l^2} \left(n + \frac{1}{2} \right) - \frac{3K}{2l^2}, \quad E_1 = \frac{B}{l^2} \left(n - \frac{1}{2} \right) - \frac{1K}{2l^2},$$

$$E_2 = \frac{B}{l^2} \left(n - \frac{3}{2} \right) + \frac{1K}{2l^2}, \quad E_3 = \frac{A}{l^2} \left(n - \frac{5}{2} \right) + \frac{3K}{2l^2}.$$

Now we have to transform this second-order differential operator into the first order one. The simplest way is to treat first derivatives ψ'_i as unknown functions. But they will not be continuous during crossing the heterointerface. The more convenient way is to build new unknown functions acting upon the wave function by the velocity operator $v_z = i/\hbar (\mathbf{H}z - z\mathbf{H})$. The continuity of function obtained is the consequence of the number of particle conservation. Substituting $\mathbf{H} = A \partial^2/\partial z^2 + B \partial/\partial z + C$ we obtain

$$v_z = \frac{i}{\hbar} \left(2A \frac{\partial}{\partial z} + B \right). \quad (5)$$

The same result with slightly different argumentation was obtained in Ref. 17. For our operator (4), formula (5) gives

$$\tilde{\psi} = \left(\begin{pmatrix} m_h^{-1} & 0 & 0 & 0 \\ 0 & m_l^{-1} & 0 & 0 \\ 0 & 0 & m_l^{-1} & 0 \\ 0 & 0 & 0 & m_h^{-1} \end{pmatrix} \frac{\partial}{\partial z} + \frac{1}{l} \begin{pmatrix} 0 & Q & 0 & 0 \\ -Q & 0 & 0 & 0 \\ 0 & 0 & 0 & -P \\ 0 & 0 & P & 0 \end{pmatrix} \right) \psi. \quad (6)$$

Now we can write the complete system of first order differential equations for the ψ and $\tilde{\psi}$ functions. The first four equations can be obtained from Eq. (6) directly, while the last four equations can be obtained by differentiating Eq. (6) and substituting the second derivatives into Eq. (4):

$$\begin{aligned}
\psi'_1 - m_h \left(\tilde{\psi}_1 - \frac{Q}{l} \psi_2 \right) &= 0, \\
\psi'_2 - m_l \left(\tilde{\psi}_2 + \frac{Q}{l} \psi_1 \right) &= 0, \\
\psi'_3 - m_l \left(\tilde{\psi}_3 + \frac{P}{l} \psi_4 \right) &= 0, \\
\psi'_4 - m_h \left(\tilde{\psi}_4 - \frac{P}{l} \psi_3 \right) &= 0, \\
\tilde{\psi}'_1 - \left[\left(A \left(n + \frac{1}{2} \right) - m_l Q^2 - \frac{3}{2} K \right) \frac{1}{l^2} + u - \epsilon \right] \psi_1 + m_l \frac{Q}{l} \tilde{\psi}_2 - \frac{N}{l^2} \psi_3 &= 0, \\
\tilde{\psi}'_2 - \left[\left(B \left(n - \frac{1}{2} \right) - m_h Q^2 - \frac{1}{2} K \right) \frac{1}{l^2} + u - \epsilon \right] \psi_2 - m_h \frac{Q}{l} \tilde{\psi}_1 - \frac{M}{l^2} \psi_4 &= 0, \\
\tilde{\psi}'_3 - \left[\left(B \left(n - \frac{3}{2} \right) - m_h P^2 + \frac{1}{2} K \right) \frac{1}{l^2} + u - \epsilon \right] \psi_3 - m_h \frac{P}{l} \tilde{\psi}_4 - \frac{N}{l^2} \psi_1 &= 0, \\
\tilde{\psi}'_4 - \left[\left(A \left(n - \frac{5}{2} \right) - m_l P^2 + \frac{3}{2} K \right) \frac{1}{l^2} + u - \epsilon \right] \psi_4 + m_l \frac{P}{l} \tilde{\psi}_3 - \frac{M}{l^2} \psi_2 &= 0,
\end{aligned} \tag{7}$$

where u is the electrostatic potential and ϵ is the energy eigenvalue.

The number n in this notation is slightly different, then used in Refs. 4–6. The more convenient numeration in our opinion was used in Ref. 18 and we also will follow this notation. We will treat the n , $n-1$, $n-2$, $n-3$ as the Landau level number N for holes states with spin $-3/2$, $-1/2$, $+1/2$, $+3/2$, respectively. These numbers correspond to index of $\varsigma_i(x, y)$ envelope function of the dominant in the $B \rightarrow 0$ limit wave function spin component. In this notation all Landau levels have four spin sublevels (two for the heavy-hole and two for the light-hole solutions). However, this is not the case in the n notation. In $n=0$ case all components except $-3/2$ one is zero. This level is a spin pure hole state. For $n=1$ we have two and for $n=2$ three nonzero components. All other states are completely mixed and have four nonzero spin components. In the $B=0$ limit all hole states are pure because only one wave function component differs from zero.

Now we have to incorporate in our system the Poisson equation on the potential u in Hartree approximation. This can be done by integrating the Poisson second order differential equation along the z direction. The wave function density integral χ can also be obtained as the solution of first order differential equation. The last equation corresponds to the energy eigenvalue ϵ :

$$\begin{cases} u' + 4\pi \frac{e^2}{\epsilon} [n_s(p_l \chi + \rho_l - 1) + N_i \times z - N_s] = 0, \\ \chi' - \psi_1^2 - \psi_2^2 - \psi_3^2 - \psi_4^2 = 0, \\ \epsilon' = 0, \end{cases} \tag{8}$$

where n_s is the 2D-hole gas surface density, ϵ is the dielectric constant, l is the energy level index, p_l is the hole density fraction, belonging to the l th energy level ($\sum p_l = 1$), χ is the wave function density integral [$\chi(z \rightarrow -\infty) = 0, \chi(z \rightarrow +\infty) = 1$], ρ_l is the wave function density integral averaged among all the rest of the energy levels,

$$\rho_l = \sum_{i \neq l} p_i \chi_i,$$

N_i is the charged impurities density in the depletion layer, N_s is the total charged impurities density in the depletion layer per unit area $N_s = W_d N_i$, and W_d is the depletion layer thickness. Here we neglect the electrostatic imaging because of the small difference in dielectric constants of GaAs and AlGaAs. In the conditions of continuous photoexcitation the hole's chemical potential lies roughly in the middle between the top of the valence band and the acceptor level, i.e., at the energy $U_h \approx 15$ meV above the top of the valence band. This fact allows us to estimate the depletion layer thickness from the first equation in Eq. (8) if we disregard the hole's charge density and assume $u(W_d) = U_h$:

$$W_d = \sqrt{\frac{U_h \epsilon}{2\pi e^2 N_i}}.$$

For $N_i \approx 10^{15} \text{ cm}^{-3}$ this leads to $W_d \approx 150 \text{ nm}$.

Before using a numerical method for solving system (7), (8) we have to restrict ourselves to some finite region along the z direction. It is very convenient to choose the region with width W_d between the heterointerface and the boundary of the depletion region, where the potential becomes constant. The potential outside the former boundary can also be treated as constant because its changing interval is much longer than wave function penetration length. In this approximation the hole's wave function $\vec{y} = \{\psi, \tilde{\psi}\}$ outside the boundary is the solution of linear differential equation $\vec{y}' + \mathbf{A}\vec{y} = \vec{0}$ with independent z matrix \mathbf{A} . This approximation can be used for building boundary conditions on the wave function. The first condition is necessary to ensure that the wave function vanishes outside the boundary. It can be written as

$$\mathbf{A}_0^+ \mathbf{y}_0 = 0, \quad \mathbf{A}_1^- \mathbf{y}_1 = 0,$$

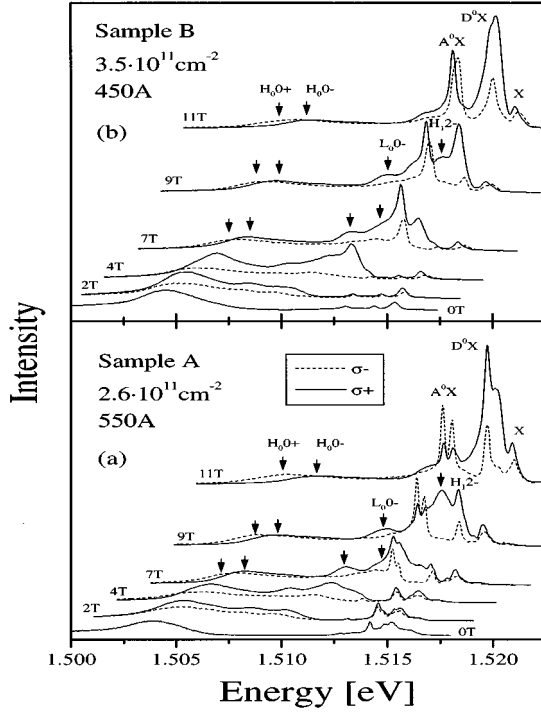


FIG. 1. Luminescence spectra, measured for two samples (A and B) in different perpendicular magnetic fields in σ^+ (solid lines) and σ^- (dashed lines) circular polarizations. The lines marked as X, A^0X , and D^0X correspond to the recombination of the free and bound excitons in the bulk GaAs.

where A_0^+ and A_1^- are two projectors into the subspaces of the A matrix with positive and negative eigenvalues real parts calculated at the left and right boundaries, respectively. The second boundary condition must represent the wave function density integral χ at the boundary. In the most general case it would be written as

$$\chi = \int \mathbf{y}^T \mathbf{D} \mathbf{y} dz,$$

where \mathbf{D} is a quadratic form matrix. So, we have to calculate

$$\int_0^\infty \mathbf{y}^T \mathbf{D} \mathbf{y} dz = \mathbf{y}_0^T \mathbf{I}_0^\infty(\mathbf{A}, \mathbf{D}) \mathbf{y}_0,$$

where \mathbf{I}_0^∞ is an unknown matrix. Using a matrix exponent representation for the wave function

$$\mathbf{y}(z) = e^{-\mathbf{A}z} \mathbf{y}_0$$

and using the partial integration procedure we can obtain the following recurrent relation which can be used for \mathbf{I}_0^∞ matrix determination with arbitrary precision:

$$\mathbf{I}_0^\infty(\mathbf{A}, \mathbf{D}) = \frac{1}{2} \mathbf{D} \mathbf{A}^{-1} + \frac{1}{2} \mathbf{I}_0^\infty(\mathbf{A}, \mathbf{D} - \mathbf{A}^T \mathbf{D} \mathbf{A}^{-1}).$$

The luminescence intensity for the l th hole level in the σ^+ and σ^- polarization can be written as

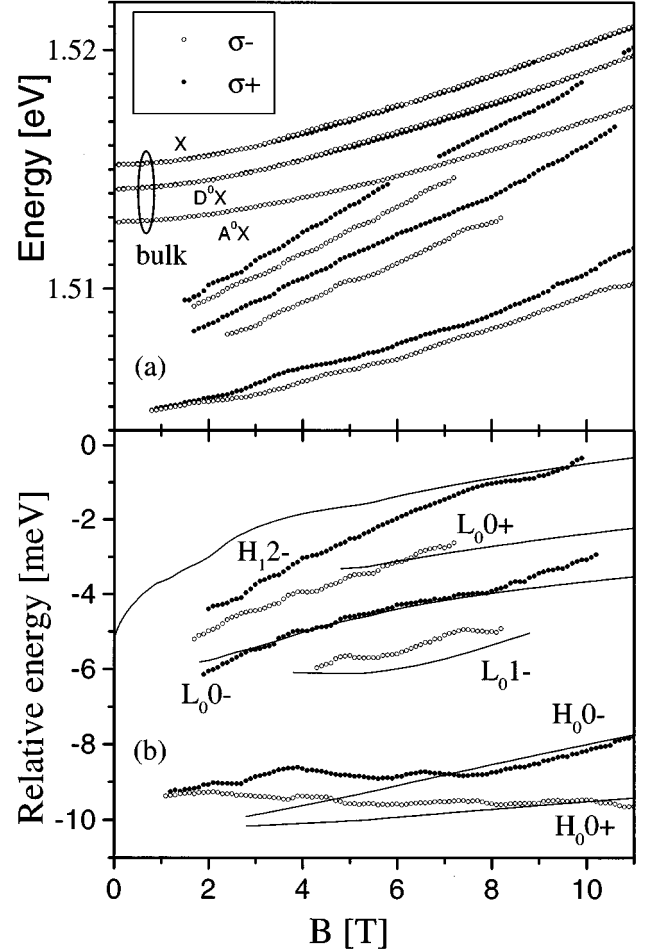


FIG. 2. (a) Magnetic field dependence of the spectral position of different luminescence lines, measured for sample A in different circular polarizations. (b) A comparison of the measured and calculated magnetic field dependence of the energy splitting between different quantum states of 2D holes.

$$\begin{cases} I_l^+ = p_l \left[\frac{3}{4} \langle \psi_1 | e_D^- \rangle + \frac{1}{4} \langle \psi_2 | e_D^+ \rangle \right], \\ I_l^- = p_l \left[\frac{3}{4} \langle \psi_4 | e_D^+ \rangle + \frac{1}{4} \langle \psi_3 | e_D^- \rangle \right], \end{cases}$$

where $|e_D^\pm\rangle$ is the electron wave function in the z direction with two different spin projections. Here we take into account that the spin matrix element for heavy holes is 3 times higher than for light holes.¹⁹ The selection rule for allowed transitions is the difference in spin being equal to ± 1 . Neglecting electron spin splitting and its polarization we can approximate the wave function of the electron bound to the donor by hydrogenlike function in the z direction

$$|e_D\rangle = e^{-|z-z_D|/a_B},$$

where z_D is the δ -layer position and a_B is the donor's Bohr radius. The matrix elements $\langle \psi_i | e_D^\pm \rangle$ then can be calculated as integrals along the z direction. The total luminescence intensity and polarization degree can be expressed as

$$I_l^\sigma = \frac{p_l}{4} [3 \langle \psi_1 | e_D \rangle + \langle \psi_2 | e_D \rangle + \langle \psi_3 | e_D \rangle + 3 \langle \psi_4 | e_D \rangle],$$

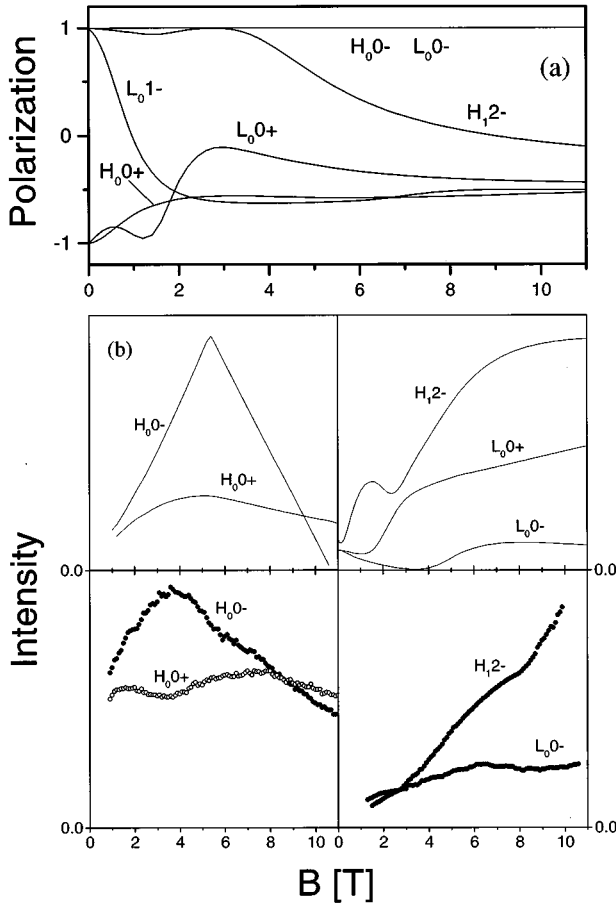


FIG. 3. (a) Magnetic field dependence of the degree of circular polarization calculated for different quantum states of 2D holes. (b) A comparison of the magnetic field dependencies of the recombination intensity measured and calculated for different quantum states of 2D holes.

$$\rho_l = \frac{I_l^+ - I_l^-}{I_l^+ + I_l^-} = \frac{3\langle\psi_1|e_D\rangle + \langle\psi_2|e_D\rangle - \langle\psi_3|e_D\rangle - 3\langle\psi_4|e_D\rangle}{3\langle\psi_1|e_D\rangle + \langle\psi_2|e_D\rangle + \langle\psi_3|e_D\rangle + 3\langle\psi_4|e_D\rangle}.$$

In our calculations we used the following Luttinger's parameters of GaAs:²⁰

$$\gamma_1 = 7.52, \quad \gamma_2 = 2.48, \quad \gamma_3 = 3.23, \quad k = 1.7.$$

IV. RESULTS AND DISCUSSION

In Fig. 1 we show the luminescence spectra, measured at $B=0$ for two different p -type single heterojunctions with a monolayer of donors located at different distances from the interface ($Z_0=55$ nm and $Z_0=45$ nm in samples A and B, respectively). One can see from this figure that at $B=0$ T, in addition to the well-known bulk lines of GaAs, new lines in the range of 1.503–1.508 eV appear in the luminescence spectra measured for these structures. As was experimentally established that the intensities of these lines considerably drop both for $Z_0>60$ nm and $Z_0<30$ nm. These observations are very similar to the results previously obtained in n -type GaAs/AlGaAs single heterojunctions with a monolayer of acceptors,²¹ however, the optimal (maximal intensity of luminescence) distance Z_0 found in these structures was considerably smaller and close to 25 nm. The established

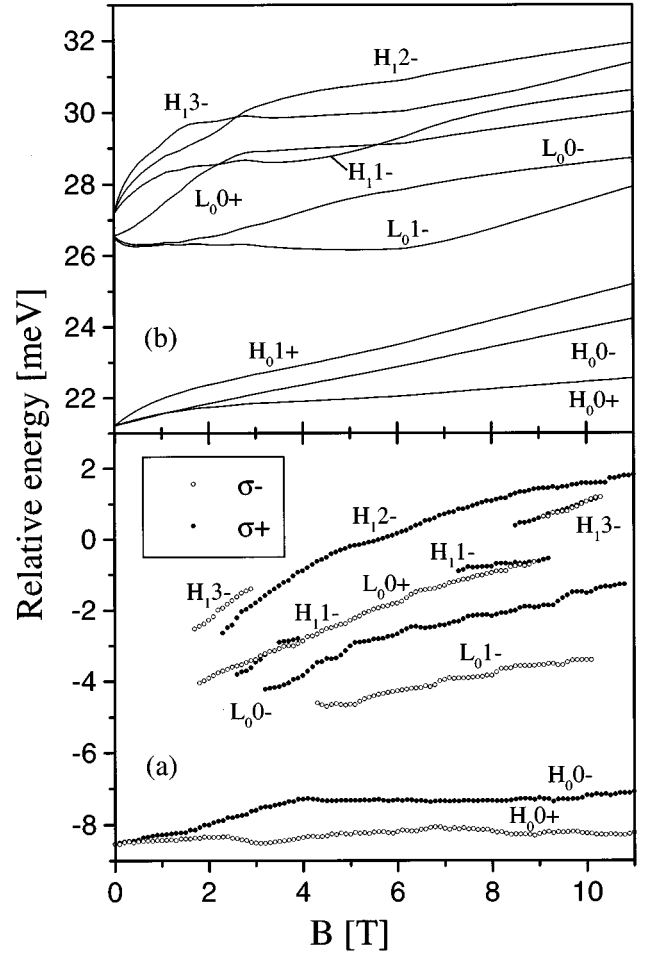


FIG. 4. A comparison of the measured (a) and calculated (b) magnetic field dependencies of the energy splitting between different quantum states of 2D holes in sample B.

difference in optimal values of Z_0 for n - and p -type GaAs/AlGaAs single heterojunctions is due to the considerably smaller Bohr radius ($a_B=3$ nm) and the larger binding energy ($Ry=28$ meV) of a neutral acceptor in comparison with the respective values of the neutral donor ($a_B=15$ nm and $Ry=5.7$ meV). In contrast to the case of recombination of 2D electrons with holes bound to acceptors, the lineshape of the luminescence associated with the recombination of 2D holes does not reflect the density of states, but its width at $B=0$ T approximately corresponds to the value of the Fermi energy of the 2D holes.

In a perpendicular magnetic field these luminescence lines split into several spectral components (see Fig. 1) which show very different behaviors of the intensity, circular polarization, and energy position as a function of the magnetic field. The magnetic field dependencies of the spectral position, measured for different luminescence lines in σ^- and σ^+ polarizations for sample A with $n_h=2.6\times 10^{11}$ cm⁻² are shown in Fig. 2(a). The lines X , D^0X , and A^0X shown in this figure correspond to the recombination of the free excitons, of the excitons bound to donors, and of the excitons bound to acceptors in the bulk GaAs. All other lines are due to the recombination of 2D holes (from different quantum states) with photoexcited electrons bound to donors from the δ layer.

In Fig. 2(b) we compare the magnetic field dependencies of the energy levels, measured experimentally from different optical transitions, with the calculated energy spectrum of 2D holes (experimental results are presented here as an energy shift from the D^0X state, in order to extract the diamagnetic shift of the neutral donor). In this figure we show only the most intensive transitions, which are enhanced due to a strong overlap of the wave functions of 2D holes and of an electron bound to the donor, located at the distance of 55 nm from the interface. These transitions correspond to a recombination from the light-hole subband [marked as L_00- , L_00+ , and L_01- in Fig. 1(b)] and from the second excited heavy-hole subband (H_12-). In spite of the fact that these subbands are not occupied under the equilibrium conditions, in optics experiments, such a hot luminescence is usually very intensive since the intersubband relaxation and recombination processes have comparable time scales. Therefore, a decrease in the population of the excited subbands can be compensated by a strong enhancement in recombination efficiency due to a stronger overlap of the wave functions. In the ground heavy holes subband we resolved only two lines associated with H_00- and H_00+ transitions.

An assignment of the experimental lines was made by a comparison of the magnetic field dependence of the spectral position, intensity and polarization of the lines. Such a comparison is presented in Fig. 3 for the H_00- , H_00+ , L_00- , and H_12- lines. It is clear from this figure that the transitions H_00- and L_00- are fully polarized in σ^+ circular polarization, whereas all other transitions H_00+ , L_00+ , L_01- , and H_12- are only partially polarized. A similar behavior of circular polarization was established for the observed luminescence lines. A rather good correspondence

was also found for the magnetic field dependencies of the intensity calculated and measured for different transitions (see Fig. 3). For the sample with a higher concentration of 2D holes we observed an even more complicated structure of the luminescence lines. The spectrum of 2D holes, measured for sample *B* with $n_h = 3.5 \times 10^{11} \text{ cm}^{-2}$, is presented in Fig. 4(a). One can see in this figure the crossing and the anticrossing of 2D-hole energy levels, the change of the sign of circular polarization and the appearance of additional quantum states of the holes. In spite of the very complicated measured magnetic field behavior of the energy levels, their polarizations, and intensities, a rather good agreement with the calculated spectrum of 2D holes [shown in Fig. 4(b)] was established.

V. SUMMARY

We have investigated the energy spectrum of two-dimensional holes in a perpendicular magnetic field in *p*-type GaAs/AlGaAs single heterojunctions by the magneto-optical method, based on the study of radiative recombination of 2D holes with photoexcited electrons bound to donors. A complex structure of both equilibrium populated heavy holes and nonequilibrium populated light holes energy levels is directly observed in the luminescence spectra and a reasonable agreement with the calculated energy spectra of 2D holes and an optical transition matrix element is established.

ACKNOWLEDGMENTS

This work was supported by DFG-grant and Russian Fund of Fundamental Research. The authors thank V. E. Bisty for useful discussions.

¹K. von Klitzing *et al.*, Phys. Rev. Lett. **45**, 494 (1980).

²D. C. Tsui *et al.*, Phys. Rev. Lett. **48**, 1559 (1982).

³E. Y. Andrei *et al.*, Phys. Rev. Lett. **60**, 2765 (1988).

⁴D. A. Broido and L. J. Sham, Phys. Rev. B **31**, 888 (1985).

⁵U. Ekenberg and M. Altarelli, Phys. Rev. B **32**, 3712 (1985).

⁶S.-R. Eric Yang, D. A. Broido, and L. J. Sham, Phys. Rev. B **32**, 6630 (1985).

⁷J. P. Eisenstein *et al.*, Phys. Rev. Lett. **53**, 2579 (1984).

⁸L. V. Butov *et al.*, Phys. Rev. B **49**, 14 054 (1994).

⁹J. Orgonasi *et al.*, J. Phys. Colloq. **48**, C5-407 (1987).

¹⁰A. G. Davies *et al.*, J. Cryst. Growth **111**, 318 (1991).

¹¹M. B. Santos *et al.*, Phys. Rev. Lett. **68**, 1188 (1992).

¹²P. J. Rodgers *et al.*, Physica B **184**, 95 (1993).

¹³H. C. Manoharan and M. Shayegan, Phys. Rev. B **50**, 17 662 (1994).

¹⁴I. V. Kukushkin and V. B. Timofeev, Adv. Phys. **45**, 147 (1996).

¹⁵I. V. Kukushkin *et al.*, Europhys. Lett. **22**, 287 (1993).

¹⁶W. H. Press *et al.*, *Numerical Recipes in C* (Cambridge University Press, Cambridge, 1992).

¹⁷R. Eppenga *et al.*, Phys. Rev. B **36**, 1554 (1987).

¹⁸B. B. Goldberg *et al.*, Phys. Rev. B **38**, 10 131 (1988).

¹⁹C. R. Pidgeon and R. N. Brown, Phys. Rev. **146**, 575 (1966).

²⁰C. Neumann *et al.*, Phys. Rev. B **37**, 922 (1988).

²¹I. V. Kukushkin *et al.*, Phys. Rev. B **40**, 7788 (1989).